We can now replace the actual bell-shaped function T by the Glaser expression for such functions, $T = \dfrac{T_m}{1+(Z/a)^2}$, having the same maximum T_m, and a half-width a such that the T^2 curves, real and model, have the same area—using formula (4.15), we see that this ensures that the focal lengths are identical in the extreme case of weak convergence. For a we obtain the expression:

$$a = -\left(\frac{1}{\pi\omega}\right)\left(\frac{1+\sqrt{\gamma}}{1-\sqrt{\gamma}}\right)^2\left[\left(\frac{1+\gamma}{1-\gamma}\log_e\gamma\right)+2\right]. \tag{8.9}$$

The values of focal length which have been calculated in this way are accurate to within two per cent for very convergent lenses in the region which is used in practice: $0{\cdot}1 < \gamma < 10$; an excellent agreement. The numerical values are obtained from the formulae:

$$f_i = \frac{a K \gamma^{-1/4}}{\sin(K\pi)}, \qquad f_0 = \frac{a K \gamma^{1/4}}{\sin(K\pi)},$$

$$z_{F_i} = a K \cot(K\pi) - \frac{T_m a^2}{4},$$

$$z_{F_0} = -a K \cot(K\pi) - \frac{T_m a^2}{4},$$

$$K = \sqrt{1+\left(\frac{3}{16}\right)a^2 T_m^2}, \tag{8.10}$$

$$a = 0{\cdot}483 \coth^2\left(\frac{x}{2}\right)(x\coth x - 1),$$

$$T_m = 2{\cdot}636 \tanh\left(\frac{x}{2}\right), \qquad x = -\log_e\sqrt{\gamma}.$$

K is always very close to unity, and the formulae approximate to:

$$\sqrt{\gamma} = 1+\varepsilon, \qquad K = 1 + 0{\cdot}0675\,\varepsilon^2\left(\frac{1}{\sqrt{\gamma}}\right), \tag{8.11}$$

$$a = 0{\cdot}644\left(1+\frac{\varepsilon^2}{10}\right), \qquad f_0 = 3{\cdot}036\frac{\gamma^{3/4}}{\varepsilon^2}.$$

The reduced ray can be written in terms of sinusoidal functions.

In Fig. 72, the closeness of the agreement between the values of the focal length calculated in this way and the values obtained experimentally by Spangenberg and Field (1943) is displayed—the other curve in the same figure represents the behaviour of the abscissa of the image focal plane.

The curve $T(Z)$ and the cardinal elements are even more accurately represented if we write

$$T = T_0 \operatorname{sech}\left(\frac{Z}{b}\right) \tag{8.12}$$

(Fig. 73); the reader is referred to the article by Bernard and Grivet (1952a) for further details. In Fig. 74, the results furnished by this improved model, the theoretical results of Goddard (1944), and the experimental results of Spangenberg and Field (1943) are all presented simultaneously for comparison.

So far we have been making the assumption that the gap between the cylinders is thin; if this gap is in fact of width $2d$, however, the axial potential is found to be well represented by

$$\eta = \frac{\Phi_1+\Phi_2}{2}\left[1+\frac{1-\gamma}{1+\gamma}\,\frac{1}{2\omega d}\log_e\frac{\cosh\omega(z+d)}{\cosh\omega(z-d)}\right], \tag{8.13}$$

so that the formulae listed earlier are still valid provided ω is replaced by ω_1, where

$$\omega_1 = \frac{\tanh(\omega d)}{d}, \qquad \omega = 1{\cdot}318. \tag{8.14}$$

These same formulae also describe quite accurately (to within a few per cent) the lens which is formed by two diaphragms in which two equal circular holes have been cut.

8.2 LENSES FORMED FROM THREE DIAPHRAGMS

8.2.1 The Potential

The three-electrode, or "einzel" lens is frequently used as the second lens of a cathode ray oscillograph, and is also the standard type of lens for an electrostatic electron microscope. As the bibliography for this paragraph shows, it has often been studied; we shall describe the properties of the einzel lens in terms of the very complete, though analytically simple, theory which Regenstreif (1951a) has proposed. We have already stated that the potential around a single plate with a circular hole, lying between two distant parallel plates without holes, can be calculated; on the axis, it takes the form

$$\Psi(z) = a + bz + c\,z\tan^{-1}\left(\frac{z}{R}\right). \tag{8.15}$$

Regenstreif, and later Bertein (1952b), have shown that the potential on the axis of the three-electrode lens can be represented approximately by a linear superposition of three potential functions of the form (8.15). We try, therefore, to use a function of the form

$$\eta(z) = A\Psi(z-z_0) + B\Psi(z) + C\Psi(z+z_0). \tag{8.16}$$

A function constructed in this way satisfies Laplace's equation exactly, but can only be approximately matched to the boundary conditions.

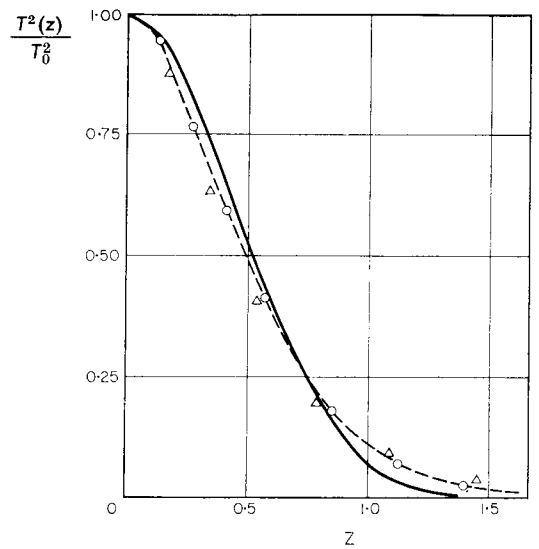

FIG. 73. Approximations to the characteristic function.
——— : the actual form of $T^2(Z)$. Δ Δ Δ : the model $T^2(Z) = \frac{T_0^2}{1 + (Z/a)^2}$.
—∘—∘— : the model $T^2(Z) = T_0^2 \operatorname{sech}^2 (Z/b)$.

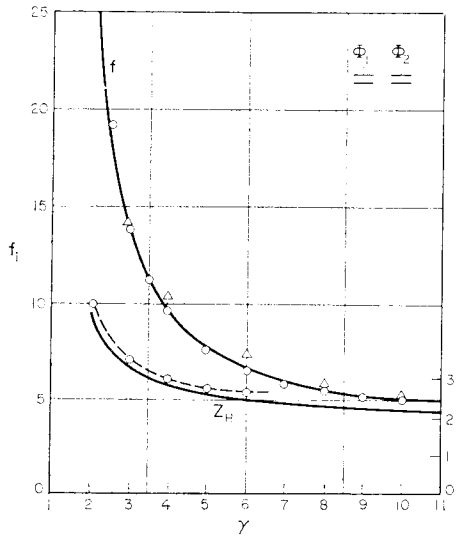

FIG. 74. The cardinal elements of lenses with two equal cylinders.
——— : results obtained with the second approximation (Grivet–Bernard).
Δ Δ Δ : experimental results. —∘—∘— : Goddard's theoretical results.

Regenstreif selected the values of A, B, C, a, b, c in such a way that $\varphi(z)$ would represent the actual field most faithfully at the centre of the lens where the electrons move most slowly, and are hence most susceptible to deviation. This produces

$$\begin{aligned} \varphi(z) &= a + b\left[(z + z_0)\tan^{-1}\left(\frac{z + z_0}{R_2}\right)\right. \\ &\qquad \left. + (z - z_0)\tan^{-1}\left(\frac{z - z_0}{R_2}\right) - 2z\tan^{-1}\left(\frac{z}{R_1}\right)\right], \\ a &= \Phi_1 - 2b\left[R_1 + z_0\tan^{-1}\left(\frac{z_0}{R_2}\right)\right], \\ b &= \frac{\Phi_2 - \Phi_1}{2R_1 + 2z_0\tan^{-1}\left(\frac{z_0}{R_1}\right)}, \end{aligned} \tag{8.17}$$

in which R_1 is the radius of the opening in the central electrode, which is held at potential Φ_1; R_2 is the radius of the opening in each of the outer electrodes, which are held at potential Φ_2; and z_0 is the distance between the central electrode and each of the other two. This notation is shown in Fig. 75a; in Figs. 75b and 75c a cross-section of the actual lens and a photograph of the actual component parts are to be seen. A potential function of the form (8.17) is not difficult to handle, and a comparison between electrolytic tank measurements and this mathematical model shows that the latter provides a very good description of the lens. We should, however, point out that a considerably less accurate model is necessary

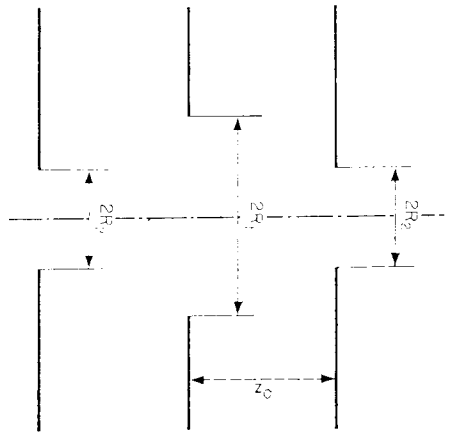

FIG. 75a. The lens formed from three thin diaphragms.

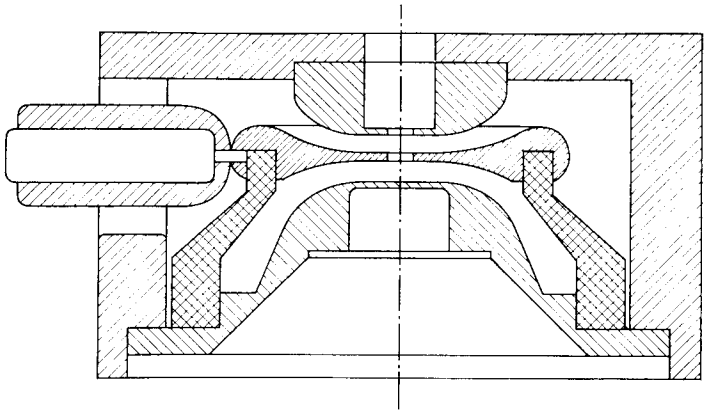

FIG. 75b. The cross-section of a three-electrode lens (scale: $^3/_5$).

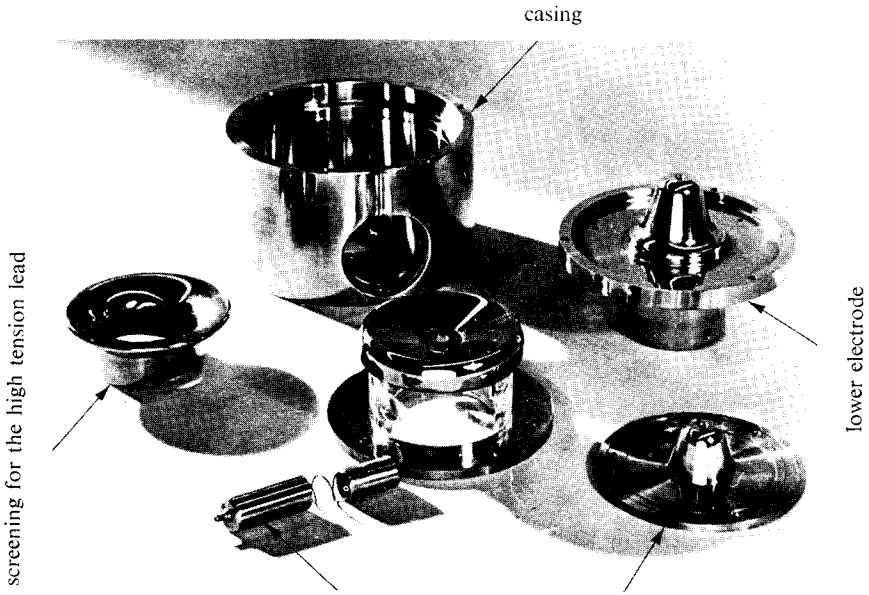

FIG. 75c. Some typical electrodes.

this case than in the case of the immersion objective which is discussed later; an error of a few per cent is of little importance, as the electron velocity never drops below some 20 per cent of the maximum velocity, whereas near a cathode, the corresponding velocity might be less than one-thousandth of its value at the anode.

In a unipotential lens with all three openings the same size, and with a thick central electrode, there is a different method of approximating to the real situation which gives a better expression for $\varphi(z)$ in the neighbourhood of the centre of the lens, particularly if the holes are large in diameter with respect to the inter-electrode distance (a situation in which Regenstreif's formulae can no longer be applied).

The general solution of the Laplace equation can be put into the form

$$\Phi(z, r) = \int_0^\infty [A(k) \sin k z + B(k) \cos k z] I_0(k r) \, \mathrm{d}k . \qquad (8.18)$$

If the potential is known over the surface of a cylinder of radius R, $A(k)$ and $B(k)$ can be determined and the axial potential $\varphi(z)$ deduced. We suppose, therefore, that the potential over the cylinder on which the peripheries of the three apertures lie varies in some simple fashion; we suppose, for example, that the potential, which is constant over the electrode surfaces, changes linearly between them, an assumption fully justified by measurements in the electrolytic tank.

With a potential Φ_2 applied to the outer electrodes and Φ_1 to the central one, the formula which is finally obtained for $\varphi(z)$ (for $z \geqq 0$) is

$$\varphi(z) = \Phi_1 - \frac{\Phi_2 - \Phi_1}{2\omega(z_2 - z_1)} \log \left[\frac{\cosh \omega(z + z_2) \cosh \omega(z - z_2)}{\cosh \omega(z + z_1) \cosh \omega(z - z_1)} \right] \qquad (8.19)$$

(see Septier (1953), for example), in which $\omega = 1{\cdot}318$, z_1 is the abscissa of the face of the central electrode, and z_2 that of the inner face of the outer electrode. The origin $z = 0$ is at the centre of the lens, and the radius of the openings is taken as the unit of length.

The case $z_1 = z_2$ corresponds to the limiting situation of a three-cylinder lens, with an infinitely small gap between each pair of cylinders. The potential reduces to

$$\varphi(z) = \Phi_1 - \tfrac{1}{2}(\Phi_2 - \Phi_1) [\tanh \omega(z + z_2) - \tanh \omega(z - z_2)]. \qquad (8.20)$$

The situation in which the diaphragms have different radii has been studied by Ehinger and Bernard (1954).

8.2.2 The Cardinal Elements

The formulae of the preceding section are too complicated to be substituted into the ray equation with any hope of successfully solving it. Regenstreif, following an idea of Rüdenberg (1948), represented the curve $\varphi(z)$ by three smoothly joined parabolic arcs. The Gaussian or transgaussian equation of motion is soluble in terms of hyperbolic functions (with arguments which are circular functions) or of circular functions (with hyperbolic functions as arguments). Each arc is joined continuously

and with the same gradient at the frontier between each parabolic region: although the calculation is long, it is straightforward and possesses the advantage that the resulting formulae are particularly tractable in that

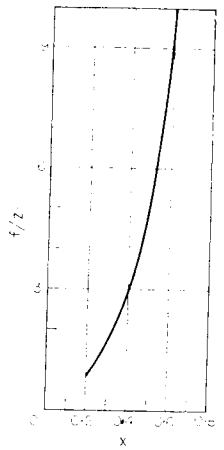

FIG. 76. The focal length of a weak lens as a function of x.

for a whole range of microscope lenses, the physical data only appear in the form of a single, and thus most convenient, parameter x, given by

$$x = \frac{\varphi(0)}{\varphi(z_0)} = \frac{\Phi_1 + \dfrac{\Phi_2 - \Phi_1}{1 + \dfrac{z_0}{R_1}\tan^{-1}\left(\dfrac{z_0}{R_1}\right)}}{\Phi_1 + (\Phi_2 - \Phi_1)\left[1 - \dfrac{\dfrac{R_2}{2R_1}}{1 + \dfrac{z_0}{R_1}\tan^{-1}\left(\dfrac{z_0}{R_1}\right)}\right]}; \quad (8.21)$$

x is simply the ratio of the axial potential at the centre, $\varphi(0)$, to the potential on the axis in the plane of one of the outer electrodes. From among Regenstreif's numerous results on this series of lenses, we list five important examples:

(i) The focal length of a lens of *weak or medium* convergence is given by

$$\frac{f}{z_0} = \frac{8}{3}\frac{x}{(1-x)^2} \quad (8.22)$$

(see Fig. 76); the principal planes then coincide with the central electrode.

(ii) The focal length f of strong lenses and the position z_F of their foci are given by

$$\frac{f}{z_0} = \frac{0{\cdot}72}{\sin(0{\cdot}707\log_e x + 0{\cdot}355)},$$

$$\frac{z_F}{z_0} = 1 + 0{\cdot}764\frac{\sin(0{\cdot}707\log_e x - 0{\cdot}887)}{\sin(0{\cdot}707\log_e x + 0{\cdot}355)} \quad (8.23)$$

(see Fig. 77).

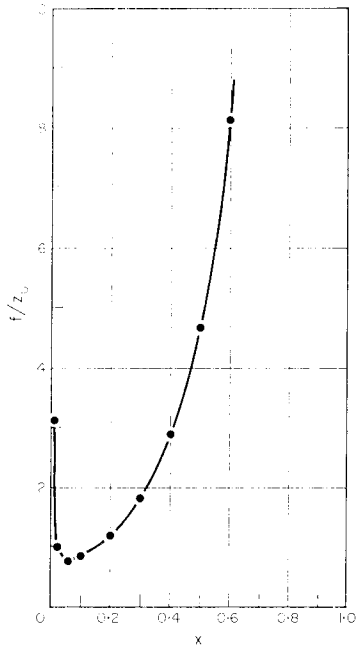

FIG. 77. The behaviour of the focal length of a strong lens.

(iii) The critical potential Φ_c of the central electrode at which the lens is transformed into a mirror is given by

$$\frac{\Phi_c}{\Phi_2} = -\frac{1}{\dfrac{z_0}{R_1}\tan^{-1}\left(\dfrac{z_0}{R_1}\right)} \quad (8.24)$$

(see Fig. 78).

(iv) The focal length of convergent or divergent mirrors is given by

$$\frac{f}{z_0} = \frac{0{\cdot}72}{\sin[0{\cdot}707\log_e(-x) + 0{\cdot}355]} \quad (8.25)$$

(see Fig. 79).

(v) The cardinal elements of lenses in which the central electrode is positive and accelerating in its action are given by Regenstreif, and the behaviour of the focal length is illustrated in Fig. 80.

The formulae which we have at our disposal, therefore, are adequate to describe very fully indeed the behaviour of this family of lenses. These theoretical predictions are in satisfactory agreement with the measurements of Heise and Rang (1949).

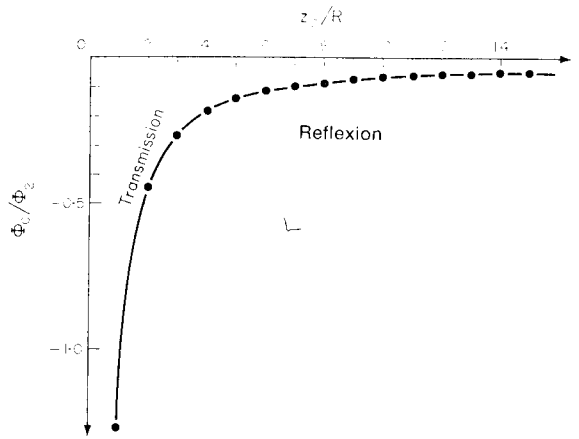

FIG. 78. The repulsive potential Φ_c/Φ_2 as a function of z_0/R_1.

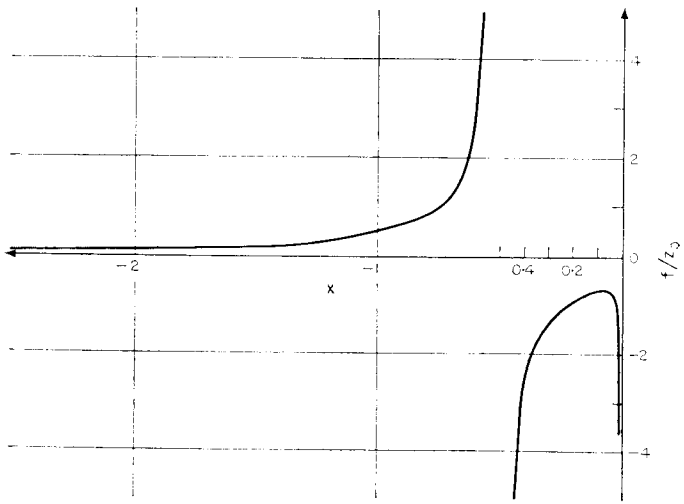

FIG. 79. The focal lengths of mirrors.

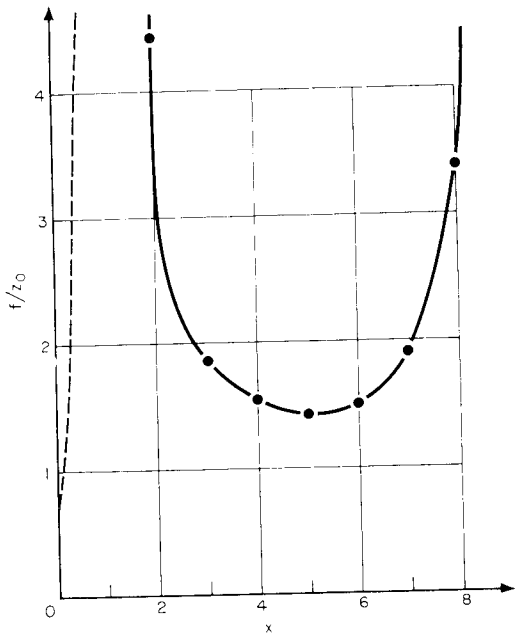

FIG. 80. The focal lengths of lenses with a positive central electrode.

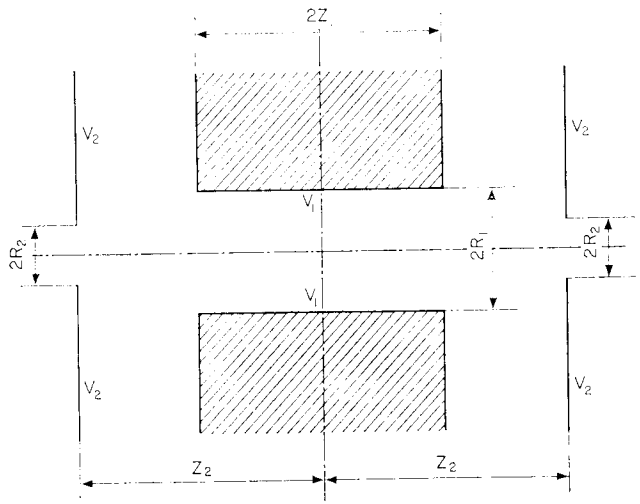

FIG. 81. The appearance of a lens with a thick central electrode.

Finally, we mention the case in which the central electrode is very thick, for which the formulae are more complicated but no more difficult—the potential is represented by a wide "plateau" in the centre of the lens, and to the parabolic arcs, we must add a fourth section, a horizontal straight line; the results are again in good agreement with experiment.

In Fig. 81, the lens is shown schematically; in Fig. 82, the values of the focal length are plotted. The parameter v is defined by $v = z_1/z_2$.

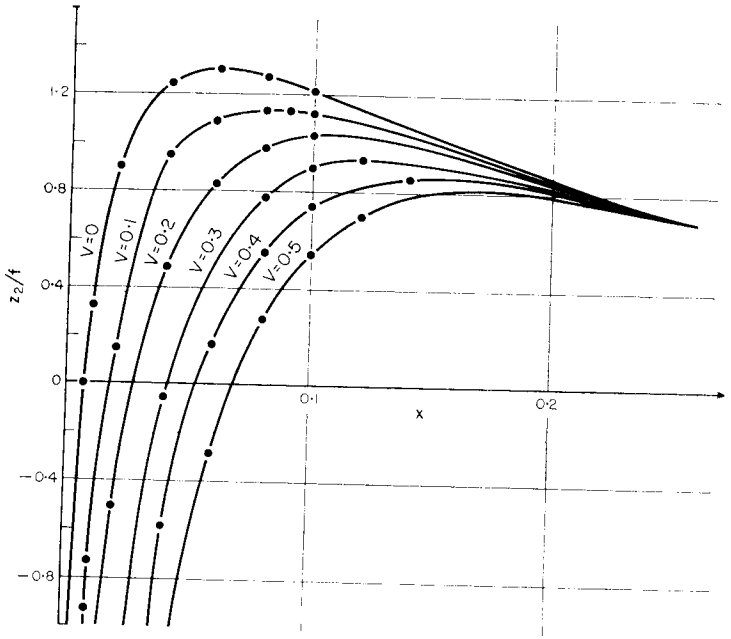

FIG. 82. The focal length of a lens with a thick central electrode as a function of x, for various thicknesses.

8.2.3 Aberrations; Ellipticity Astigmatism

The results of the preceding section have a special relevance when we consider aberrations, since the focal length, distortion, and spherical aberration all pass through their minima simultaneously (Bruck and Romani, 1944; Heise, 1949). With the aid of Regenstreif's formulae, therefore, we can easily establish the conditions for these minima which correspond to the value $x_m = 5{\cdot}8 \times 10^{-2}$ ($f_m = 0{\cdot}7730$) when the central electrode is thin. Only with difficulty can the aberration coefficients C_s and C_c of the lens be determined using this approximate method; we need to represent $\Phi(z)$ by a single, well-chosen, analytic function, which would enable us to integrate the equation of the paraxial rays. Glaser (1952) and Glaser

and Schiske (1954, 1955) have suggested the following model:

$$\Phi_0(z) = \Phi_0 - \frac{\Phi(O)}{1+(z/d)^2} = \Phi_0\left(1 - \frac{k^2}{1+(z/d)^2}\right),$$

with

$$k^2 = \frac{\Phi(O)}{\Phi_0}.$$

Φ_0 denotes the accelerating voltage and d is the half-width of the bell-shaped curve representing $\Phi(z)$; $\Phi_0(O) = \Phi_0 - \Phi(O)$ is the potential at $z = 0$ (Fig. 82a).

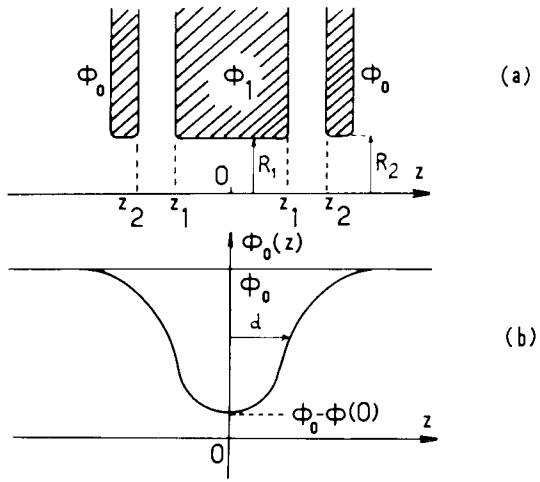

FIG. 82a. The potential distribution in an einzel (unipotential) lens, the Glaser–Schiske model: d denotes the half-width at half the maximum height.

The factor k^2 can be calculated by Regenstreif's method, recently improved by Kanaya *et al.* (1966), for each type of lens and each value of Φ_1. The following table gives the values of k^2 and d for various lenses, when the central electrode is held at cathode potential ($\Phi_1 = 0$).

R_1/R_2	z_1/R_1	z_2/R_1	k^2	d/z_2
		1	0·550	0·875
1	0	2	0·740	0·677
		4	0·860	0·590
2	0	2	0·720	0·615
		4	0·855	0·581
	1	3	0·950	0·700
1	1·5	3·5	0·980	0·705
	1·5	4·5	0·988	0·659
	2	4	0·996	0·750